International Journal of Thin Films Science and Technology

http://dx.doi.org/10.18576/ijtfst/100313

Effect of Mn Doped and Mn+Sn Co-doping on the Properties of ZnO Thin Films

K. Salim [1,*], *W. Azzaoui* [1], *M. N. Amroun* [1] *and A. H. Kacha* [2]

[1] Laboratoire d'Elaboration et de Caractérisation des Matériaux, département d'électronique, Université Djilali Liabes, BP89, Sidi Bel Abbés 22000. Algeria
[2] Laboratoire de Micro-electronique Appliquee, Universite Djillali Liabes, 22000 Sidi Bel Abbes, Algeria

Received: 21 Jan. 2021, Revised: 25 Feb. 2021, Accepted: 19 May 2021.
Published online: 1 Sep. 2021.

Abstract: Mn doped and Mn/Sn co-doped ZnO thin films nanoparticles have been successfully synthesized by Spray pyrolysis technique at 300 ^{0}C. X-ray diffraction study showed that all the films have the hexagonal wurtzite structure with the preferential orientation (002) plane. The optical measurement exhibited an increase in the average transmittance from 77% for Mn doped ZnO to 84% for Mn/Sn co-doped ZnO films in the visible region. Further the optical band gap changes from 3.18 eV for undoped ZnO films to 3.27 eV for Mn/Sn co-doped ZnO films. The electrical resistivity has decreased with incorporation of Mn and Sn ions to reach the minimum value of 11 (Ω.cm) for Mn doped ZnO films.

Keywords: ZnO, thin films, spray pyrolysis.

1 Introduction

Semiconducting metal oxides, such as SnO_2, CdO and ZnO are commonly employed in resistive gas sensors, exploiting the changes in the electrical conductivity of these materials upon expo-sure to gaseous mixtures **[**1,2**].** Among these metal oxides, zinc oxide thin film has attracted much attention due to its interesting properties such as high optical transparency in the visible region and wide band gap, non-toxicity and good adherence to many substrates for this is considered one best candidates in a variety of applications including light emission devices, laser diodes, solar cells, photo-detectors, transparent electronics, piezoelectric devices, spin electronics **[**5**].** It was used in chemo-resistive sensors to detect several gases, such as H2, NH3, CH4, O2, ethanol and CO **[**3,4**].** Zinc oxide (ZnO) is an n-type semiconductor with wide band gap (3.37eV) and high excitation bonding energy (60 meV) **[**6**].** It is important to report that doping and/or co-doping ZnO films with other elements
strongly affects its physical properties. Typical dopants that have been used to produce conducting films of ZnO belong to the group III elements (B, Al, In, Ga), IV elements (Pb, Sn) and VII elements (Mn, Tc) of the periodic table. In this study, Mn doped ZnO (MZO) and Mn/Sn co-doped ZnO (MTZO) thin films were synthesized by spray pyrolysis technique. The Structural, optical and electrical properties of the deposited films have been investigated.

The X-ray analysis of prepared films were Recorded by Bruker D2 PHASER X-Ray Diffractometer (CuKα radiation, λ = 1.5406 Å) radiation 2θ range of 20–70°, The optical transmittance was recorded in the wavelength range from 300 to 2500 nm using JASCO 570 type UV-visible-NIR double-beam spectrophotometer. Finally, the electrical properties are measured with ECOPIA HMS-5000 Hall Effect system at room temperature.

2 Experimental Details

Mn doped and Mn + Sn co-doped ZnO thin films were deposited by spray pyrolysis technique with Mn concentration 4 at.% and different Sn concentrations 2 and 4 at.% respectively. The starting solution was prepared by dissolving Zinc chlorid (0.1 M) ($ZnCl_2$. $2H_2O$) in double distilled water, Magnesium chloride tetrahydrate $MnCl_2.4H_2O$ and Tin chloride dihydrate $SnCl_2.2H_2O$ with 0.1M as the dopant precursors. The other condition of deposition, such as substrate temperature 300˚C, solution volume sprayed 100 ml, nozzle-substrate distance 30 cm. The substrates were cleaned in ultrasonic bath with ethanol for 5 min and washed with double distilled water to remove and clean surface impurities. After the process of growth, the coated substrates were allowed to cool naturally to room temperature.

*Corresponding author E-mail: karim22000@hotmail.com

3 Results and Discussion

3.1 Structural Properties

X-ray diffraction pattern of undoped, Mn doped and Mn + Sn co-doped ZnO thin films shown in Fig 1(a). The fig 1(a) shows that diffracted peaks appeared at 2θ = 32.12°,34.77° ,36.56°, 47.80°, 56.87°,63.14° and 68.24° peaks corresponding to the (100), (002), (101), (102), (110), (103) and (112) planes respectively. All the samples exhibit a hexagonal wurtzite structure (JCPDS No. 36-1451). No additional peaks were detected in the XRD diagrams corresponding to Mn_2O_3 or SnO_2 crystals or another phase, suggesting that the incorporation of Mn and Sn elements into the ZnO lattice does not affect its crystal structure phase. The preferred orientation (002) plane decreases with Mn/Sn addition which suggest decrease in crystal quality of the films (see Table 1). Moreover, a slight shift of the (002) peak towards lower 2-theta degrees was observed fig 1(b) indicates a uniform state of stress with tensile components parallel to c-axis.

The average crystallite

$$D = \frac{0.9\lambda}{\beta cos\theta} \quad (1)$$

Where D is the crystallite size, λ used (1.5406 Å), β is the (FWHM) of the peak (200) and θ is the Braggs angle. It observed that the crystallites size of the films reduces with Mn and Sn addition.

The lattice parameters (a) and (c), The micro-strain (ε) and The dislocation density of the prepared thin films are determined by the following relations, **respectively [6,7].**

The lattice parameters (a) and (c), The micro-strain (ε) and The dislocation density of the prepared thin films are determined by the following relations, respectively [6,7].

$$\frac{1}{d^2} = \frac{4}{3}\left(\frac{h^2+hk+k^2}{a^2}\right) + \left(\frac{l^2}{c^2}\right) \quad (2)$$

$$\varepsilon = \frac{\beta cos\theta}{4} \quad (3)$$

$$\delta = \frac{1}{D^2} \quad (4)$$

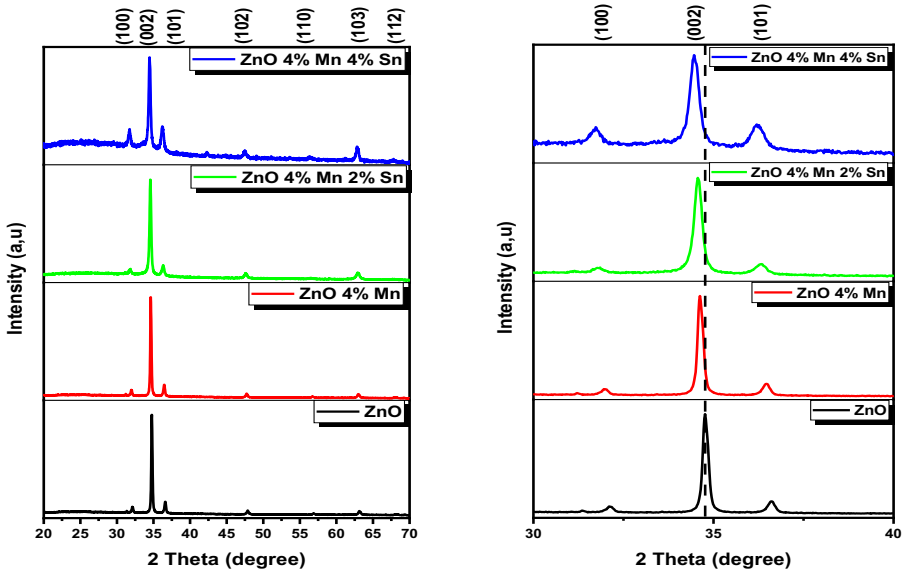

Fig 1: XRD patterns of undoped, Mn doped and Mn+Sn co-doped ZnO films.

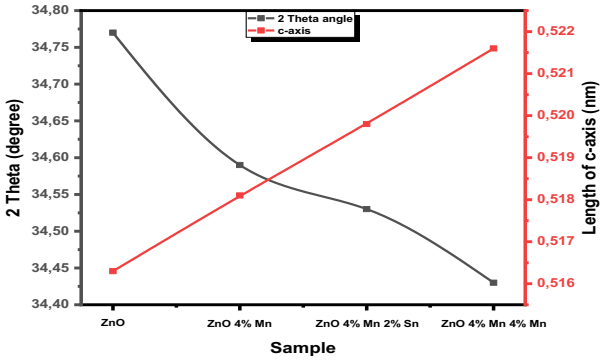

Fig 2: Variation of 2 Theta values of the (002) XRD peak and length of c-axis of undoped, Mn doped and Mn+Sn co-doped ZnO films.

Table 1: Structural parameters of of undoped, Mn doped and Mn+Sn co-doped ZnO films.

Sample	$2\theta^{\circ}_{(002)}$	FWHM $.10^{-3}(\beta)$	Grain size D (nm)	d (002)	a (Å)	c (Å)	ε Strain $.10^{-4}$	Dislocation density $.10^{-4}$ Line/nm^2
ZnO pure	34.76	3.66	39.69	2.578	3.210	5.163	8.73	6.34
ZnO 4% Mn	34.62	4.28	33.93	2.588	3.223	5. 181	10.21	8.68
ZnO 4%Mn 2% Sn	34.56	4.75	30.57	2.593	3.239	5.198	11.33	10.70
ZnO4% Mn 4% Sn	34.46	5.74	23.07	2.600	3.248	5.216	13.70	18.78

Table 1 illustrates the effect of Mn doped and Mn+Sn co-doped on the structure parameters of ZnO films evaluated from the XRD data. It is observed that the length of c-axis increases gradually with incorporation of Mn and Sn elements (see **Fig 2**), indicated that the divalent Mn^{2+} and Sn^{+4} ions substituted for Zn^{2+} ions in ZnO crystal lattice. Moreover, the line width of (002) diffraction peaks was found to be gradually broadened and shifted to lower 2-theta degrees (see **Fig 1(b)**), this is presumably due to lattice disorder and strain induced by Mn^{2+} and Sn^{+4} ions substitution .

3.2 *Optical properties*

Fig 3 shown the optical transmittance in the wavelength range of 350-2500 nm of undoped, Mn doped and Mn + Sn co-doped ZnO thin films deposited on glass substrates. The average optical transmittance for the films is > 77%. It can be observed that the transparency of the films increases from 77% for undoped films to 84% for (4% Mn + 4% Sn) co-doping ZnO films in the visible and NIR region, which suggest that Mn+Sn co-doping enhances the transmittance of the ZnO films indicating good incorporation of the Mn+Sn elements in the ZnO lattice structure. The optical band gap (Eg) of the films can be determined by the Tauc law expression [8]:

$$(ahv)^n = A(hv - Eg) \quad (5)$$

Where α is the absorption coefficient, hv the photon energy, A constant and Eg the optical band gap. We take n=2 for direct band gap semiconductors.

It can be found (**Table 2**) that the optical band gap increases with addition of Mn and Sn elements, reaching maximum of about 3.27 eV for Mn 4%+ Sn4% at co-doped ZnO films. Generally, the absorption spectra of semiconductors are largely altered bu dopants. This change in the energy band gap can be explained by two competing phenomena [9,10,11].

1. The first phenomenon is called the Burstein Moss shift: The doping creates degenerate energy levels with band-filing that causes the Fermi level to move above the conduction band edge. This phenomenon induces an increase in the band gap with the doping concentration.
2. The doping results in the rise of addition band tail states, leading to shrinkage of the band gap. This phenomenon becomes dominant above a threshold concentration and corresponds to the increase of the disorder introduced by doping.

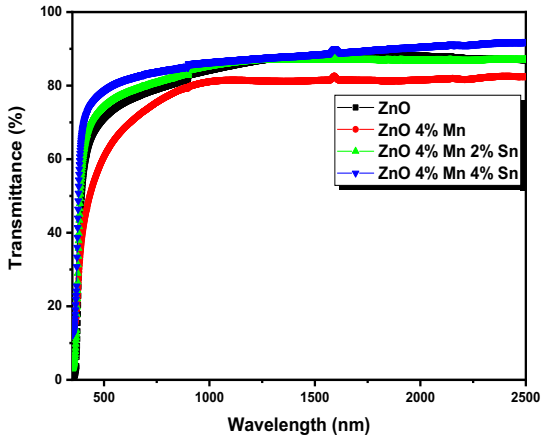

Fig. 3: Variation of optical transmittance with wavelength.

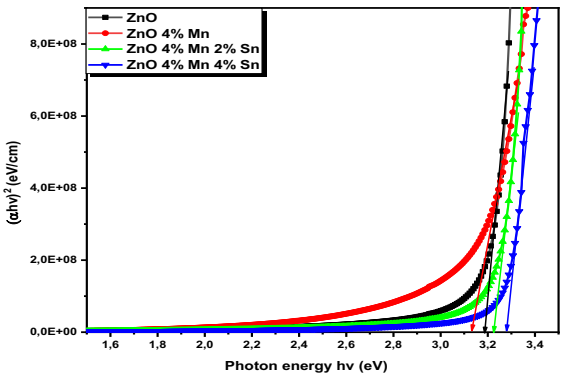

Fig.4: Variation of $(\alpha h\upsilon)^2$ with photon energy.

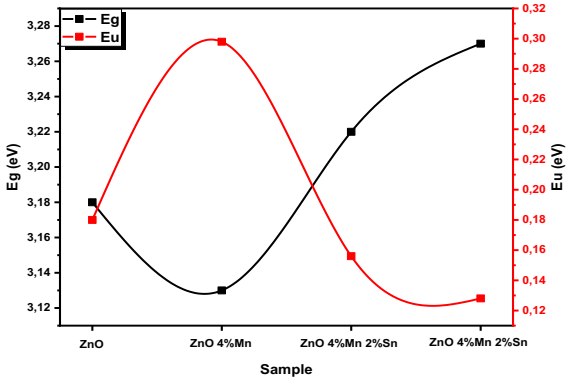

Fig. 5: Variation of Band gap energy and Urbach energy with ZnO pure, Mn doped and Mn+Sn co-doped. with Mn+Sn.

temperature. The obtained results are presented in **Table 3**. The negative sign of carrier concentrations confirms that n-type conductivity. The carrier concentration of undoped ZnO films is $-3.66.10^{+16}$ cm^{-3} The increase in carrier concentration with Mn and Sn addition may be originate from the replacement of Zn^{2+} ions by Mn^{2+} and Sn^{4+} ions in ZnO lattice and the substitution can liberate free electrons in the conduction band. High value of the resistivity was observed for undoped ZnO films of 109 Ωcm. It observed that the resistivity of the films decreased with Mn doped and Mn+Sn co-doped due to the increase in the carrier concentration. As the ionic radius of Sn^{+4} (0.69 Å) is smaller than that of Zn^{2+} (0.74 Å), the chance for Sn^{4+} to substitute Zn^{2+} in the ZnO lattice becomes higher. When Sn^{4+} substitutes Zn^{2+} sites in the ZnO matrix, it provides two free electrons to the system for electric conduction.

Table 2: The optical band gap and Urbach energy of ZnO pure , Mn doped and Mn+Sn co-doped.

Sample	Eg (ev)	Eu (eV)
ZnO pure	3.18	0.180
ZnO 4% Mn	3.13	0.298
ZnO 4%Mn 2% Sn	3.22	0.156
ZnO 4% Mn 4% Sn	3.27	0.128

3.3 Electrical Properties

Table 3: Electrical properties of the prepared thin films.

Sample	Mobilité (cm^2/VS)	Carrier Concentrations (cm^{-3})	Résistivité (Ω.cm)	Sheet Resistance (Rsh) (MΩ/sq)
ZnO pure	$1.79.10^{-01}$	$-3.66.10^{+16}$	109	5.45
ZnO 4% Mn	$7.37.10^{-01}$	$-9.54.10^{+17}$	11.1	0.51
ZnO 4%Mn 2% Sn	$3.13.10^{-01}$	$-5.57.10^{+17}$	19.6	1.28
ZnO 4% Mn 4% Sn	$5.96.10^{-01}$	$-6.65.10^{+17}$	18.9	1.09

The carrier concentration (n), mobility (μ) and resistivity (ρ) of the undoped, Mn doped and Mn + Sn co-doped ZnO thin films were measured using Hall Effect at room

4 Conclusions

Undoped, Mn doped and Mn+Sn Co-doped ZnO thin films were deposited by spray pyrolysis with different tin

contents on glass substrates at constant substrate temperature of 300 °C.

The XRD analysis showed (002) peak as the preferred orientation and exhibited wurtzite structure for all the films. The 4% Mn+ 4% Sn co-doped ZnO film has the highest transmittance of 84%. The optical band gap of the films increases with incorporation of Mn and Sn concentrations. The investigated electrical properties of deposited thin films have demonstrated that Mn doping and Mn+Sn co-doping improved the carrier concentration and resistivity of ZnO thin films.

References

[1] T.Seiyama, S. Kagawa, Study on a detector for gaseous components using semi-conductive thin films, Anal. Chem., **38**, 1069-1073, 1966.

[2] G.Sberveglieri, G. Faglia, S. Groppelli, P. Nelli, Methods for the preparation ofNO, NO2and H2sensors based on tin oxide thin films, grown by means of ther.f.magnetron sputtering technique, Sens. Actuators B., **8**, 79-88, 1992.

[3] B. Bott, T.A. Jones, B. Mann, The detection and measurement of CO using ZnOsingle crystals, Sens. Actuators., **5**, 65-73, 1984.

[4] J.D.Choi, G.M. Choi, Electrical and CO gas sensing properties of layeredZnO–CuO sensor, Sens. Actuators., **B 69**,120-126, 2000.

[5] J. Yoo, J. Lee, S. Kim, K. Yoon, I. Jun Park, S.K. Dhungel, B. Karunagaran, D. Mangalaraj, Y. Junsin, High transmittance and low resistive ZnO:Al films for thin film solar cells, Thin Solid Films **480**, (213-217), 2000

[6] S.K. Dhungel, B. Karunagaran, D. Mangalaraj, Y. Junsin, High transmittance and low resistive ZnO:Al films for thin film solar cells, Thin Solid Films., **480**,(213-217), 200.

[7] M.N.Amroun, K. Salim, A. H. Kacha and M. Khadraoui,Effect of TM (TM= Sn, Mn, Al) Doping on the Physical Properties of ZnO Thin Films Grown by Spray Pyrolysis Technique: A comparative Study, Int. J. Thin. Film. Sci. Tec., **9**, 1, 2020.

[8] M.N.Amroun , K. Salim , A. H. Kacha and M. Khadraoui, Tco's Thin Films Grown By Spray Pyrolysis Technique For Window Layer Of Solar Cell Application: A Comparative Study, Int. J. Thin.Film. Sci. Tec., **9**, 103-110, 2020.

[9] M.N.Amroun, K. Salim and A. H. Kacha , Molarities Effect on Structural Optical and Electrical Properties of Nanostructured Zinc Oxide deposited by Spray Pyrolysis Technique, Int. J. Thin. Fil. Sci. Tec., **10**, 67-73, 2021.

[10] Burstein E.Anomalous optical absorption limit in InSb. Phys. Rev., **93** , 632, 1954.

[11] Kim CE et al. Effect of carrier concentration on optical band gap shift in ZnO:Ga thin films. Thin solid films., **518**, 6307, 2010.

[12] Leary K et al, disorder and optical absorption in amorphous silicon and amorphous germanium. J Non-Cryst Solids ., **210**, 249-253,1997.

[13] M. N. Amroun, A. H. Kacha , K. Salim and M.Khadraoui, Investigations In Structural Morphological And Optical Properties Of Cd1-Xsnxs Thin Films, Int. J. Thin.Film. Sci. Tec., **9**, 89-102, 2020.